Letter

Signature of glassy dynamics in dynamic mode decompositions

Zachary G. Nicolaou,[1,2,3,*] Hangjun Cho,[4,5,6] Yuanzhao Zhang,[7] J. Nathan Kutz,[1,8,5] and Steven L. Brunton[4,5]
[1]*Department of Applied Mathematics, University of Washington, Seattle, Washington 98195, USA*
[2]*Department of Physics & Astronomy, University of Tennessee, Knoxville, Tennessee 37996, USA*
[3]*Department of Mathematics, University of Tennessee, Knoxville, Tennessee 37996, USA*
[4]*Department of Mechanical Engineering, University of Washington, Seattle, Washington 98195, USA*
[5]*AI Institute in Dynamic Systems, University of Washington, Seattle, Washington 98195, USA*
[6]*Research Institute of Mathematics, Seoul National University, Seoul 08826, Republic of Korea*
[7]*Santa Fe Institute, Santa Fe, New Mexico 87501, USA*
[8]*Department of Electrical and Computer Engineering, University of Washington, Seattle, Washington 98195, USA*

(Received 22 July 2025; accepted 22 April 2026; published 28 May 2026)

Glasses are traditionally characterized by their rugged landscape of disordered low-energy states and their slow relaxation towards thermodynamic equilibrium. Far from equilibrium, dynamical forms of glassy behavior with anomalous algebraic relaxation have also been noted, for example, in networks of coupled oscillators. Due to their disordered and high-dimensional nature, such systems have been difficult to study theoretically, but data-driven methods are emerging as a promising alternative that may aid in their analysis. Here, we characterize glassy dynamics using the dynamic mode decomposition, a data-driven spectral computation that approximates the Koopman spectrum. We show that the gap between oscillatory and decaying modes in the Koopman spectrum vanishes in systems exhibiting algebraic relaxation, and thus, we propose a model-agnostic signature for robustly detecting and analyzing glassy dynamics. We demonstrate the utility of our approach through both a minimal example of a one-dimensional ODE and a high-dimensional example of coupled oscillators.

DOI: 10.1103/ng8q-ttyb

Quantitative characterization of glassy behavior is a longstanding scientific challenge. In material physics, glasses occur in systems with a plethora of nearly degenerate low-energy configurations, leading to slow relaxation towards equilibrium, spatial disorder, and hysteresis. Frustration, wherein disharmonious interactions prevent system components from simultaneously realizing their lowest-energy configurations, often leads to glassy behavior. Progress has been made in characterizing the thermodynamics of some glassy systems such as spin glasses [1,2], but significant challenges remain, especially in systems far from equilibrium.

Dynamical analogs of glassy behavior have long attracted interest in oscillatory systems, for example, in the frozen vortex glass of the complex Ginzburg-Landau equation [3,4]. In networks of coupled oscillators, Daido first detailed a system [5] in which the dynamics relax toward an incoherent attractor at a slow, algebraic rate, in stark contrast to the exponential relaxation typically observed for attractors in dynamical systems. More recently [6], Ottino and Strogatz revisited Daido's model and recognized challenging, high-dimensional features in the dynamics in the glassy regime and a related and interesting volcano transition [7–9]. In this Letter, we propose a general strategy to detect glassy dynamics and nonexponential relaxation using the dynamic mode decomposition (DMD) [10–15], a data-driven framework for characterizing nonlinear dynamical systems by approximating the associated, infinite-dimensional Koopman and Perron-Frobenius linear operators [16–27] (see Supplemental Material, Sec. S1 A [28]). DMD has shown remarkable success in a variety of applied and theoretical studies [10,11,13,29,30] and is also being explored in the study of coupled oscillators [31–37]. Such glassy dynamics can be hidden in high-dimensional data and might be easy to miss from conventional analyses, especially if one lacks *a priori* knowledge of a good order parameter with which to quantify the scaling. In these cases, our DMD analysis offers a principled and system-agnostic way to extract algebraic relaxation dynamics from high-dimensional data.

Specifically, we note a key signature of glassy dynamics in the Koopman spectrum, as illustrated schematically in Fig. 1. For bounded systems, the Koopman spectrum can be divided into an oscillatory component, whose (continuous-time) eigenvalues are purely imaginary, and a decaying component, whose eigenvalues lie in the left half-plane (see Supplemental Material, Sec. S1 B [28]). If a gap exists between the oscillatory and the decaying modes, the relaxation towards the long-term behavior will eventually be dominated by the leading decaying mode with the smallest decay rate $-\mathrm{Re}(\mu)$. However, if this gap vanishes and there is an accumulation of decaying modes approaching the oscillatory component, other asymptotic behaviors are possible.

In the case of a vanishing gap, appropriate scaling between the mode amplitude and the vanishing decay rate can enable the cumulative response of exponentially decaying modes to give rise to algebraic relaxation. For example, Ogielski and Stein propose to decompose a power law into an infinite number of exponentially decaying modes [38]. Mathematically,

*Contact author: znicolao@utk.edu

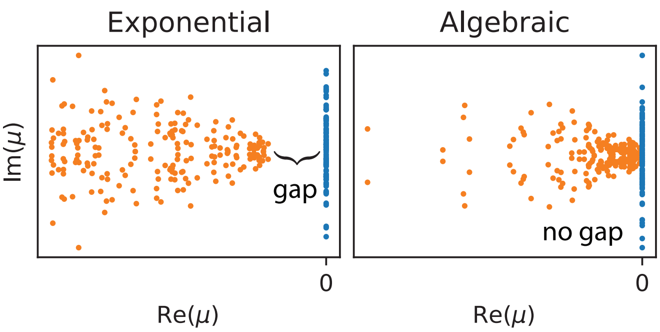

FIG. 1. Schematic of Koopman oscillatory (blue) and decaying (orange) eigenvalues for systems exhibiting exponential (left) and algebraic (right) decay. The signature absence of a gap in the spectrum allows one to detect glassy dynamics.

they show that the infinite sum $P(t) = \sum_{m=0}^{\infty} w_m e^{-\lambda_m t}$ asymptotes to $P(t) \sim t^{-\alpha} - O(e^{-t}/t)$ as $t \to \infty$ if we set $w_m = 2^{-m}$ and $\lambda_m = \frac{c(2-c)}{1-c} c^m$, where $\alpha = \frac{\log 2}{\log c^{-1}} > 0$ and $0 < c < 1$ are constants. Thus, observing a similar scaling in the DMD spectrum, which approximates the Koopman spectrum, and DMD mode amplitudes can serve as a principled way to determine if glassy dynamics are present in the data.

For clarity of presentation, we demonstrate our results first on an idealized one-dimensional system before focusing in detail on the high-dimensional Daido glassy oscillator model. We demonstrate how the glassy signature enables the development of a data-driven order parameter characterizing the transition to glassy behavior based on the distribution of DMD eigenvalues. Finally, we discuss potential applications and extensions for other systems.

Our bespoke DMD Python code leverages the dask package [39], which divides prohibitively large linear algebra operations into manageable chunks that can be performed sequentially while efficiently utilizing the available system memory. All the numerical results and data in this Letter can be reproduced from our GitHub repository [40].

Dynamic mode decomposition. We first briefly outline the DMD methods employed in our analyses. DMD gives a matrix approximation $\mathbb{K}$ of the Koopman operator corresponding to a dynamical system $\dot{x} = f(x)$, which is the infinite-dimensional linear composition operator governing the temporal evolution of measurement functions (see Supplemental Material, Sec. S1 A [28]). We are interested in the continuous case here, but data is typically available for a temporal discretization. The state x here may be a scalar, a vector, or a spatiotemporal field. We generate multiple solution trajectories $x^j(t)$, indexed by the superscript j, in an effort to sample the state space well. In the extended DMD approach [41] that we employ, we introduce a dictionary of measurements $\mathcal{D} = \{g_1, \dots, g_d\}$ in which we seek to observe this linear dynamics, where $g_i : \mathcal{M} \to \mathbb{C}$ are observable functions of the state variables and $\mathcal{M}$ is the state space. We consider the evolution of the vector composed of the dictionary evaluated on the data $\vec{\mathcal{D}}(x^j(t))$, concatenated over all trajectories, where the trajectories are sampled in time steps of size dt. The matrix $\mathbb{K}$ is the optimal linear solution for the time-varying dynamics of the dictionary terms; $\vec{\mathcal{D}}(x^j(t+dt)) \approx \mathbb{K}\vec{\mathcal{D}}(x^j(t))$. The quality of these approximations and their convergence depend on how close the span of the dictionary terms is to a Koopman invariant subspace [42,43] and on how well the data represents the full dynamics of the state space [44].

The DMD analysis produces an eigendecomposition of the matrix $\mathbb{K} = \Phi\Lambda\Phi^{-1}$, where $\Phi = [\phi_{\lambda_1}, \dots, \phi_{\lambda_d}]$ is the invertible matrix of eigenvectors (whose matrix elements we will denote by Φ_i^k) and $\Lambda = \mathrm{diag}(\lambda_1, \dots, \lambda_d)$ is the diagonal matrix of eigenvalues, which can be used to approximate Koopman functions as $\phi_i(x) = \sum_k \Phi_i^k g_k(x)$. We can then evaluate the time evolution of the mode amplitudes $b_i^j(t) \equiv \phi_i(x^j(t))$, which are expected to evolve exponentially according to $b_i^j(t) \approx b_i^j(0)e^{\mu_i t}$, where $\mu_i = \log(\lambda_i)/dt$ is the continuous-time eigenvalue. If the approximations are good, the mode amplitudes will indeed evolve exponentially, and the evolution of the dictionary terms can then be reconstructed as $\hat{g}_k(x^j(t)) \approx \sum_i \tilde{\Phi}_k^i b_i^j(0)e^{\mu_i t}$ where $\tilde{\Phi}_k^i$ are the matrix elements of the inverse Φ^{-1} (which is also the matrix whose rows are the left eigenvectors of $\mathbb{K}$). Truncated reconstructions can be used to significantly compress the data required to represent the dynamics, provided the fit is good (i.e., the mode amplitude evolution is, in fact, exponential).

The basic version of extended DMD described above suffers from issues such as spectral noise in practical applications. To mitigate these issues, we employ two extensions of the method. First, we use the exact DMD approach [45], which reduces the numerical dimension of the problem (and thus reduces the impacts of finite precision) by first projecting the analysis onto a minimal set of principal modes given by the singular value decomposition. We also employ the residual DMD (resDMD) approach [46,47], which evaluates the quality of each mode through a residual that vanishes for true Koopman modes. The resDMD analysis also enables us to evaluate pseudospectra approximating the norm ε of the resolvent of the Koopman operator, which diverges exactly on the Koopman spectrum. The pseudospectrum can help to identify neighborhoods close to Koopman eigenvalues even when the actual Koopman mode does not lie in the span of the dictionary.

Algebraic decay in a minimal example. We now consider the DMD analysis in a one-dimensional system given by

$$\dot{\theta} = -\sin(\theta)^{\zeta}. \tag{1}$$

This example clearly illustrates the difference between exponential relaxation ($\zeta = 1$) and algebraic relaxation ($\zeta = 3$). The only attractor for this system is $\theta = 0$. It is easy to show analytically that the state decays asymptotically according to $\theta(t) \sim e^{-t}$ for $\zeta = 1$ and $\theta(t) \sim t^{-1/2}$ for $\zeta = 3$ and that, under regularity assumptions on the Koopman eigenfunctions, a gap is present in the Koopman spectrum only in the $\zeta = 1$ case (see Supplemental Material, Sec. S2 A [28]).

We employ an extended resDMD analysis with a dictionary composed of Fourier-based measurements $g_k(\theta) \equiv e^{\imath k\theta}$ for integers k with $-d \leqslant k \leqslant d$ (where $\imath$ is the imaginary unit), which can approximate arbitrary square-integrable 2π-periodic functions well for large d. We perform the fit with combined data from 5 trajectories $\theta_j(t)$ with initial conditions $\theta_j(0)/\pi = (0.5, 0.4, 0.3, 0.2, 0.1)$. We confirm that the input trajectories for both $\zeta = 1$ and $\zeta = 3$ can be success-

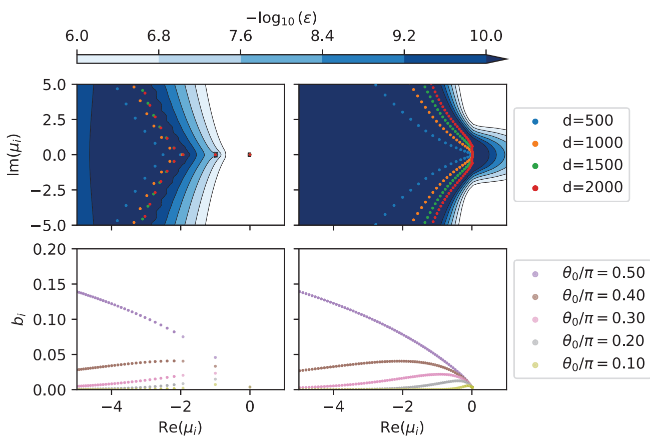

FIG. 2. DMD spectrum and pseudospectrum (top panels) and mode amplitudes vs decay rate (bottom panels) for Eq. (1) with $\zeta = 1$ (left panels) and $\zeta = 3$ (right panels). Only in the $\zeta = 3$ spectrum do we observe the glassy DMD signature (i.e., an accumulation of decaying modes approaching the imaginary axis).

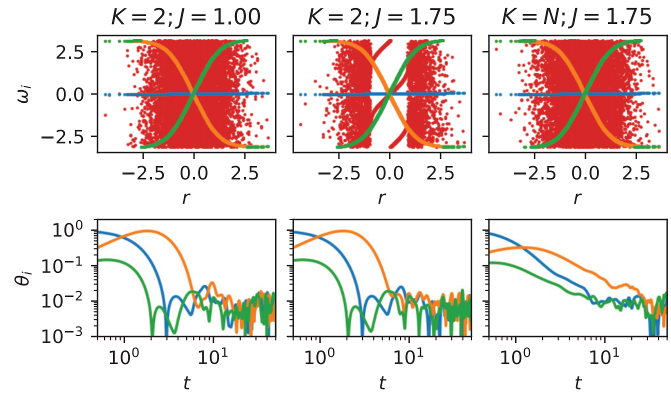

FIG. 3. Dynamics of three systems of $N = 10\,000$ oscillators in Eq. (2) with various coupling constants and rank, as indicated above each column. Top panels show oscillator phases vs natural frequency for the initial conditions for each training trajectory (blue, orange, and green dots) and the final state (red dots), and bottom panels show Kuramoto order parameter vs time for each training trajectory. The low-rank systems ($K = 2$) exhibit exponential relaxation, while the high-rank system ($K = N$) exhibits algebraic relaxation.

fully reconstructed from the initial mode amplitudes and the approximate Koopman modes (see Supplemental Material Sec. S2 B [28]), suggesting that our dictionary is sufficiently expressive.

We turn next to the qualitative features of the DMD spectrum in the two cases, as shown in Fig. 2. Since the asymptotic state for Eq. (1) is a fixed point, there is no oscillatory component, and the DMD spectrum consists only of decaying modes with $\mathrm{Re}(\mu) < 0$. As noted above, the algebraically decaying trajectories are well approximated by a sum of exponentially decaying Koopman modes, even though any finite sum of exponentially decaying terms will eventually decay exponentially. This apparent contradiction can be resolved by noting that the number of terms required in the exact Koopman representation may diverge provided the amplitudes decay sufficiently fast and the sum converges, as depicted in Fig. 1.

Indeed, the key difference between the spectra in Fig. 2 is the presence of a gap between the imaginary axis and the spectrum in the exponential case. When the gap vanishes, we also observe an associated widening and bulging of the pseudospectrum around the imaginary axis. Incidentally, we note that in the study of numerical instabilities, pseudospectral bulges like the one seen in Fig. 2 have also been related to algebraic growth [48]. Finally, in the algebraically decaying case, we observe a scaling between the initial mode amplitudes $b_i^j(0)$ and the decay rate $-\mathrm{Re}(\mu)$ that enables the sum of exponential terms to approximate an algebraic decay (see Supplemental Material, Sec. S2 B [28]), in contrast to the exponential case, where the leading mode quickly dominates.

Algebraic decay in the oscillator glass. We next consider the generalized Daido model of an oscillator glass proposed in Ref. [6],

$$\dot{\theta}_n = \omega_n + J \sum_{m=1}^{N} A_{nm} \sin(\theta_m - \theta_n), \tag{2}$$

which describes the evolution of N-coupled phase oscillators with frequencies ω_n (sampled here from a standard normal distribution), J represents the coupling constant, and $A_{nm} \equiv \sum_{k=1}^{K} (-1)^k u_k^{(n)} u_k^{(m)}/N$ are the components of a random adjacency matrix for a given even integer $K > 0$. Here, $u_k^{(n)}$ are the components of a K-dimensional random vector with each element independent and equal to ± 1 with equal probability. In the large N limit, K is the rank of the adjacency matrix. Since the signs of the adjacency matrix elements are random, the couplings include both attractive and repulsive terms, leading to frustration. In the low-rank regime, an interesting volcano transition has been characterized by a low-dimensional Ott-Antonsen reduction [49,50]. However, Daido's glassy states appear only in the high-rank regime, where no dimension reduction is available.

We implement an efficient GPU integration scheme to generate data from $N = 10\,000$ coupled oscillators at different combinations of coupling constants and adjacency matrix ranks. Our simulations enable us to investigate larger systems than previously studied, and we note a few new results about the large N systems in Sec. S3 A of the Supplemental Material [28]. Different relaxation behaviors are observed in various parameter regimes, as shown in Fig. 3. We produce trajectories from three initially ordered states that relax towards disordered states. These initial conditions consist of identical initial phases $\theta_n(0) = 0$ and initial phases with a single winding around the circle $\theta_n(0) = \pm(-\pi + 2\pi n/N)$, where the oscillator index is ordered by the natural frequencies. The Kuramoto order parameter

$$r = \left| \frac{1}{N} \sum_{n=1}^{N} e^{\imath \theta_n} \right| \tag{3}$$

has traditionally been used to quantify the relaxation. For low-rank systems with a low coupling strength (left column in Fig. 3), initial conditions decay exponentially towards an incoherent state. For low-rank systems above the critical coupling threshold (middle column in Fig. 3), interesting volcano clusters appear in the final state, but the relaxation remains ex-

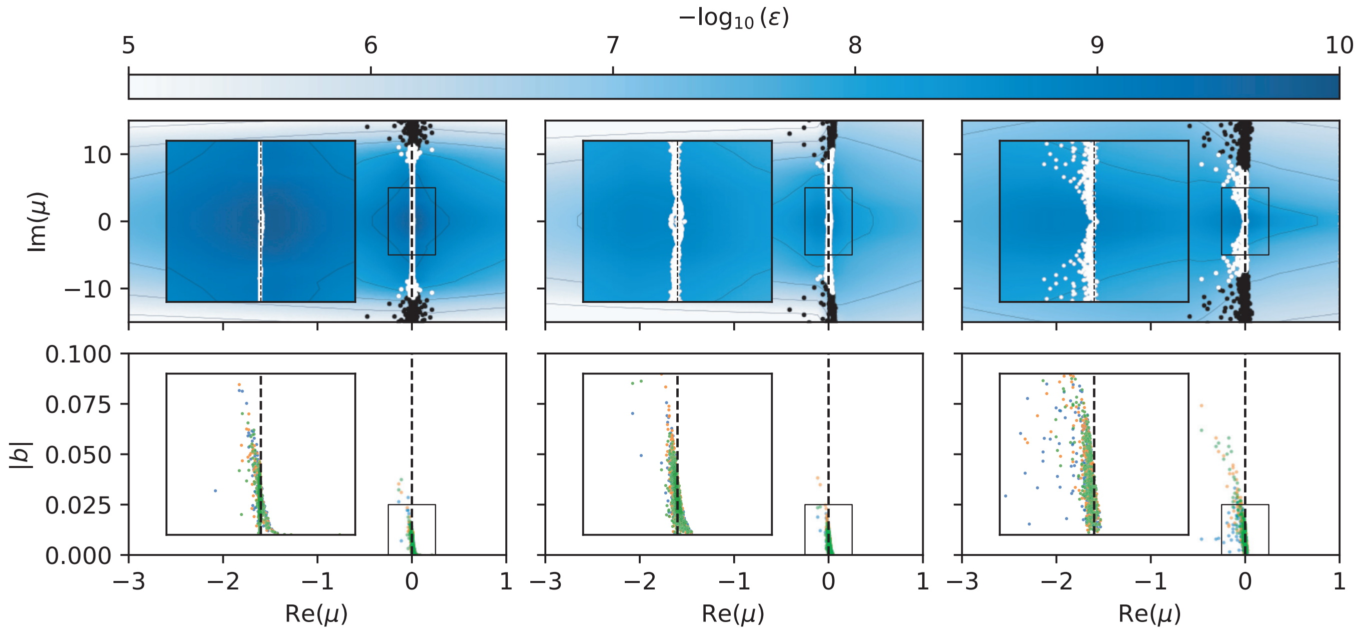

FIG. 4. DMD spectra for the three systems in Fig. 3 with $K = 2$, $J = 1.00$ (left panels), $K = 2$, $J = 1.75$ (middle panels), and $K = N$, $J = 1.75$ (right panels). In the top panels, the white dots show nonspurious DMD eigenvalues that pass the resDMD criteria $\varepsilon < 5 \times 10^{-8}$, black dots show spurious DMD eigenvalues, and blue shading shows the approximate ε pseudospectra. Insets show a zoom of the boxed portions (continuous black lines) near the imaginary axis (dashed black lines). Bottom panels show the mode amplitude $|b_i^j|$ vs decay rate $\mathrm{Re}(\mu_i)$, with color corresponding to the trajectories in Fig. 3. The spectrum is confined to the imaginary axis in the low rank ($K = 2$) cases, but the glassy signature of accumulating decaying modes is present in the high rank ($K = N$) case.

ponential. Finally, for high-rank systems with a large coupling constant (right column in Fig. 3), the slow relaxation toward incoherence follows a power law, exhibiting glassy dynamics.

We can again express arbitrary periodic measurement functions with Fourier basis elements $g_{\nu_k}(\theta) = e^{\imath \sum \nu_k \theta_k}$ for each multi-index $\nu_k \in \mathbb{Z}^N$. Indeed, in the uncoupled ($J = 0$) case, each Fourier basis element g_{ν_k} is an exact oscillatory Koopman eigenfunction with eigenvalue $\mu_{\nu_k} = \imath \sum_k \nu_k \omega_k$ (see Supplemental Material Sec. S3 B [28]). We base our extended DMD dictionary on this basis, but the high dimensionality of the state space imposes significant limitations on our dictionary. We restrict our dictionary to include only some of the lowest-order multi-indices. To enable us to study the dependence with increasing dictionary size, we include those Fourier modes with $\nu_k = \pm m\delta_k^n$, where δ_k^n is the Kronecker delta, $n = 1, 2, \cdots, N$, and $m = 1, 2, \cdots M$, leading to $2NM$ dictionary terms. We also include a random selection NM of pairwise terms of the form $\nu_k = \pm(\delta_{i(k)}^n - \delta_{j(k)}^n)$, where $i(k)$ and $j(k)$ are sampled from all pairs of distinct choices without replacement, leading to a total dictionary size of $D = 3NM$ terms. Figure 4 shows our results for the largest dictionary considered with $D = 150\,000$ terms for the three trajectories from Fig. 3. Since the attractors are not steady states, we expect the presence of oscillatory modes in the Koopman spectra, which we indeed observe in the resDMD approximations close to the imaginary axis.

Qualitative differences between the results for the exponentially relaxing cases and the glassy, algebraic relaxation are apparent in the results, but the interpretation is somewhat confounded by spectral noise in the DMD approximation of the Koopman spectrum. Nevertheless, we can clearly observe the convergence of the oscillatory component of the spectrum to the imaginary axis as the dictionary size increases (see Supplemental Material Sec. S3 C [28]). Only in the glassy case with algebraic decay (right column in Fig. 4) do we see an additional accumulation of decaying modes near the imaginary axis that do not converge to the imaginary axis as the dictionary size increases. Indeed, the DMD spectrum faithfully captures the exponential and algebraic behavior in the reconstruction of the Kuramoto order parameter,

$$\hat{r}^j(t) = \left| \sum_{i,k} \frac{1}{N} \tilde{\Phi}_k^i b_i^j(0) e^{\mu_i t} \right|, \tag{4}$$

and thus the DMD reconstruction can effectively represent the glassy dynamics observed in the oscillator system. To avoid overfitting and to mitigate spectral noise in the reconstruction, we include only the minimum necessary number of small-residue modes to reconstruct the Kuramoto order parameter to a relative accuracy of 10^{-3}, with a residue threshold of $\varepsilon < 5 \times 10^{-8}$ (white dots in Fig. 4).

It is interesting to note that in the nonglassy regimes (left two columns in Fig. 4), the DMD spectrum does not appear to include any decaying modes and consists instead of a large number of purely oscillatory modes. The incoherent summation of these oscillator modes can nevertheless give rise to an exponential relaxation towards the incoherent state. This can occur via the generalized Landau-damping phenomenon noted previously in the nonlinear Fokker-Planck description of the Kuramoto system [51], where an analytical continuation argument reveals "fake" (decaying) eigenvalues responsible for the decay. (We note an explicit relationship between our DMD spectrum and the nonlinear Fokker-Planck equation in the Supplemental Material, Sec. S3 D [28].) In the glassy regime, on the other hand, we do observe the signature of a large number of decaying DMD modes accumulating near the imaginary axis. Crucially, in both the glassy and non-glassy regimes, we emphasize that the distribution of decaying modes in our order-parameter reconstruction reproduces the observed exponential and algebraic decay rates very accurately (see Supplemental Material, Sec. S3 C [28]).

While the asymptotic behavior in the Kuramoto order parameter has traditionally been used to assess the potential for glassy dynamics, several issues have become apparent that have complicated analysis, stymied development in the literature, and led to contentious and unproductive discussions. Since only finite-size systems can be computationally simulated, the thermodynamic asymptotic relaxation is only approximately observed over a finite time window before the Kuramoto order parameter approaches the finite-size noise floor. Thus, the exact location in parameter space delimiting the glassy dynamical behavior has remained obscured. Rather than using the DMD reconstruction of the Kuramoto order parameter in Eq. (4), we introduce a new, data-driven order parameter, which better quantifies the onset of glassy dynamics in the oscillator glass. Our data-driven order parameter η is simply given by the average negative real part of the DMD eigenvalues that pass the residual DMD criteria $\varepsilon < 5 \times 10^{-8}$ (i.e., the white dots in Fig. 4),

$$\eta \equiv -\langle \mathrm{Re}(\mu_i) \rangle|_{\varepsilon_i < 5\times 10^{-8}}. \tag{5}$$

While we would prefer to evaluate η using the exact Koopman spectrum, in practice, we can only calculate the DMD eigenvalues, which, as noted above, are close to but not exactly equal to the Koopman eigenvalues. Given this source of spectral noise, some DMD eigenvalues actually appear to the right of the imaginary axis, implying a "forbidden" exponentially growing DMD mode in a bounded system. Such eigenvalues can even pass the residual DMD test as long as the inverse of their positive real part is small compared to the time length of the input trajectories. We can thus take the average real part of those positive DMD eigenvalues as a crude estimate for the spectral uncertainty for the individual eigenvalues, which we divide by the square root of the number of eigenvalues included in the mean and use to construct random error bounds for the order parameter.

Figure 5 shows the order parameter η vs the rank K of the network for two systems with different coupling constants. Note that the order parameter η is typically slightly larger than zero (black dashed line in Fig. 5) even for small-rank systems. We attribute this nonzero value to systematic errors in the DMD spectrum due to finite-size effects, including the fact that the span of the finite dictionary terms does not exactly contain any Koopman invariant subspaces and the trajectories only span a finite time. These systematic errors appear to be conservatively bounded by a window of size equal to the smallest detectable decay rate $1/T$ determined by the time span of the input trajectories (grey dashed lines in Fig. 5). It is clear that the order parameter is nonzero for systems with sufficiently large rank, and, furthermore, that this onset of the glassy dynamics occurs at a larger rank when the coupling constant is smaller. Thus, the transition to glassy decay can be quantitatively delimited using our data-driven order parameter.

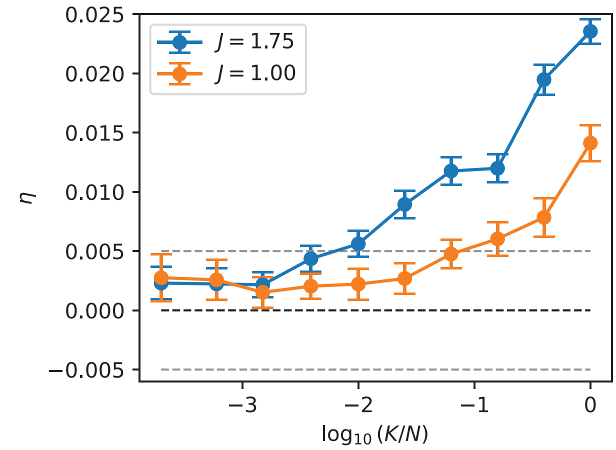

FIG. 5. Data-driven order parameter η vs logarithmic rank $\log_{10}(K/N)$, signaling the onset of glassy dynamics. Error bars show the estimated order-parameter random error bounds derived from the average of the DMD eigenvalues with positive real parts, and the gray dashed lines show the more conservative finite-size systematic error bounds.

Discussion. Leveraging a key feature in the Koopman spectrum (the presence or absence of a spectral gap), the dynamic mode decomposition and pseudospectral estimates can be utilized to define a data-driven order parameter for distinguishing exponential and algebraic dynamical relaxation, as relevant in the study of glassy systems far from equilibrium. Our results support previous findings [5,6] of glassy dynamics in Daido's frustrated oscillator model, which were only established through significant domain expertise and specialized knowledge of coupled oscillators. While we focused on Daido's oscillator glass here for clarity, the approach of deriving order parameters from DMD spectrum or other data-driven methods can be relevant to other systems as well, and we expect it may be fruitfully applied in the study of, e.g., other disordered systems of oscillators [52] and neural networks [53,54]. This work contributes to the growing body of literature utilizing data-driven approaches for qualitative system characterization [22,30,32,47,55,56].

One central challenge in our approach is the uncertainty inherent in the DMD estimates of the Koopman spectrum, which obscures the distinction between the oscillatory and decaying parts of the spectrum. Future studies would benefit from better theoretical bounds for quantifying the uncertainty of the DMD estimates. Bootstrapping or bagging estimates of the uncertainty may aid in this regard. Finally, we note that other data-driven techniques, such as applying DMD eigenvalue constraints [57], physics-informed constraints [58], and sparse system identification [59], could prove useful in future studies.

Acknowledgments. The authors gratefully acknowledge Steven H. Strogatz and Matthew J. Colbrook for insightful discussions related to this work. Funding was provided by the Washington Research Foundation Postdoctoral Fellowship (Z.G.N.), the National Research Foundation of Korea (NRF) grant funded by the Korea government (MSIT) (Grant No. RS-2023-00253171) (H.C.), the Santa Fe Institute Omidyar Fellowship and National Science Foundation (NSF Grant No.

DMS 2436231) (Y.Z.), and the National Science Foundation AI Institute in Dynamic Systems (Grant No. 2112085) (H.C., J.N.K., S.L.B.).

Data availability. The data that support the findings of this article are openly available [40].

[1] M. Mézard, G. Parisi, and M. A. Virasoro, *Spin Glass Theory and Beyond: An Introduction to the Replica Method and Its Applications* (World Scientific Publishing Company, River Edge, 1987).

[2] M. Mézard and G. Parisi, The cavity method at zero temperature, J. Stat. Phys. **111**, 1 (2003).

[3] C. Brito, I. S. Aranson, and H. Chaté, Vortex glass and vortex liquid in oscillatory media, Phys. Rev. Lett. **90**, 068301 (2003).

[4] Z. G. Nicolaou, H. Riecke, and A. E. Motter, Chimera states in continuous media: Existence and distinctness, Phys. Rev. Lett. **119**, 244101 (2017).

[5] H. Daido, Quasientrainment and slow relaxation in a population of oscillators with random and frustrated interactions, Phys. Rev. Lett. **68**, 1073 (1992).

[6] B. Ottino-Löffler and S. H. Strogatz, Volcano transition in a solvable model of frustrated oscillators, Phys. Rev. Lett. **120**, 264102 (2018).

[7] A. Prüser, S. Rosmej, and A. Engel, Nature of the volcano transition in the fully disordered Kuramoto model, Phys. Rev. Lett. **132**, 187201 (2024).

[8] D. Pazó and R. Gallego, Volcano transition in populations of phase oscillators with random nonreciprocal interactions, Phys. Rev. E **108**, 014202 (2023).

[9] S. Lee, Y. Jeong, S.-W. Son, and K. Krischer, Volcano transition in a system of generalized Kuramoto oscillators with random frustrated interactions, J. Phys. A **57**, 085702 (2024).

[10] C. W. Rowley, I. Mezić, S. Bagheri, P. Schlatter, and D. S. Henningson, Spectral analysis of nonlinear flows, J. Fluid Mech. **641**, 115 (2009).

[11] P. J. Schmid, Dynamic mode decomposition of numerical and experimental data, J. Fluid Mech. **656**, 5 (2010).

[12] J. N. Kutz, S. L. Brunton, B. W. Brunton, and J. L. Proctor, *Dynamic Mode Decomposition: Data-Driven Modeling of Complex Systems* (SIAM, Philadelphia, 2016).

[13] S. L. Brunton, M. Budišić, E. Kaiser, and J. N. Kutz, Modern Koopman theory for dynamical systems, SIAM Rev. **64**, 229 (2022).

[14] M. J. Colbrook, The multiverse of dynamic mode decomposition algorithms, Handb. Numer. Anal. **25**, 127 (2024).

[15] S. E. Otto and C. W. Rowley, Koopman operators for estimation and control of dynamical systems, Annu. Rev. Control Robot. Auton. Syst. **4**, 59 (2021).

[16] L. D. Landau and E. M. Lifshitz, *Statistical Physics: Volume 5* (Elsevier, Amsterdam, Netherlands, 1980).

[17] B. O. Koopman, Hamiltonian systems and transformation in Hilbert space, Proc. Natl. Acad. Sci. USA **17**, 315 (1931).

[18] R. K. Singh and J. S. Manhas, *Composition Operators on Function Spaces* (Elsevier, Amsterdam, Netherlands, 1993).

[19] I. Mezić, Spectral properties of dynamical systems, model reduction and decompositions, Nonlinear Dyn. **41**, 309 (2005).

[20] M. Budišić, R. Mohr, and I. Mezić, Applied Koopmanism, Chaos **22**, 047510 (2012).

[21] A. Mauroy and I. Mezić, Global stability analysis using the eigenfunctions of the Koopman operator, IEEE Trans. Automat. Contr. **61**, 3356 (2016).

[22] E. M. Bollt, Q. Li, F. Dietrich, and I. Kevrekidis, On matching, and even rectifying, dynamical systems through Koopman operator eigenfunctions, SIAM J. Appl. Dyn. Syst. **17**, 1925 (2018).

[23] A. L. Bruce, V. M. Zeidan, and D. S. Bernstein, What is the Koopman operator? A simplified treatment for discrete-time systems, in *Proceedings of 2019 American Control Conference (ACC)* (Philadelphia, PA, 2019), p. 1912.

[24] A. Mauroy, Y. Susuki, and I. Mezic, *Koopman Operator in Systems and Control* (Springer International Publishing, Berlin, 2020).

[25] I. Mezić, Spectrum of the Koopman operator, spectral expansions in functional spaces, and state-space geometry, J. Nonlinear Sci. **30**, 2091 (2020).

[26] M. Morrison and J. N. Kutz, Solving nonlinear ordinary differential equations using the invariant manifolds and Koopman eigenfunctions, SIAM J. Appl. Dyn. Syst. **23**, 924 (2024).

[27] M. J. Colbrook, I. Mezić, and A. Stepanenko, Limits and powers of Koopman learning, arXiv:2407.06312.

[28] See Supplemental Material http://link.aps.org/supplemental/10.1103/ng8q-ttyb for additional details, derivations, and simulation results.

[29] P. J. Schmid, Dynamic mode decomposition and its variants, Annu. Rev. Fluid Mech. **54**, 225 (2022).

[30] A. Rupe and J. P. Crutchfield, On principles of emergent organization, Phys. Rep. **1071**, 1 (2024).

[31] C. W. Curtis and M. A. Porter, Detection of functional communities in networks of randomly coupled oscillators using the dynamic-mode decomposition, Phys. Rev. E **104**, 044305 (2021).

[32] Y. Hashimoto, M. Ikeda, H. Nakao, and Y. Kawahara, Data-driven operator-theoretic analysis of weak interactions in synchronized network dynamics, arXiv:2208.06186.

[33] J. Hu and Y. Lan, Koopman analysis in oscillator synchronization, Phys. Rev. E **102**, 062216 (2020).

[34] A. Mauroy, I. Mezić, and J. Moehlis, Isostables, isochrons, and Koopman spectrum for the action–angle representation of stable fixed point dynamics, Physica D **261**, 19 (2013).

[35] Y. Susuki and I. Mezic, Nonlinear Koopman modes and coherency identification of coupled swing dynamics, IEEE Trans. Power Syst. **26**, 1894 (2011).

[36] D. Wilson, Data-driven identification of dynamical models using adaptive parameter sets, Chaos **32**, 023118 (2022).

[37] V. Thibeault, B. Claveau, A. Allard, and P. Desrosiers, Kuramoto meets Koopman: Constants of motion, symmetries, and network motifs, arXiv:2504.06248.

[38] A. T. Ogielski and D. L. Stein, Dynamics on ultrametric spaces, Phys. Rev. Lett. **55**, 1634 (1985).

[39] Dask Development Team (2016), *Dask: Library for Dynamic Task Scheduling*, http://dask.pydata.org.

[40] Data and code required to reproduce all results in this paper are available at our GitHub repository, https://github.com/znicolaou/kuramoto_dmd.

[41] M. O. Williams, I. G. Kevrekidis, and C. W. Rowley, A data–driven approximation of the Koopman operator: Extend-

ing dynamic mode decomposition, J. Nonlinear Sci. **25**, 1307 (2015).

[42] S. E. Otto and C. W. Rowley, Linearly recurrent autoencoder networks for learning dynamics, SIAM J. Appl. Dyn. Syst. **18**, 558 (2019).

[43] M. Haseli and J. Cortés, Temporal forward–backward consistency, not residual error, measures the prediction accuracy of extended dynamic mode decomposition, IEEE Control Syst. Lett. **7**, 649 (2022).

[44] M. Korda and I. Mezić, On convergence of extended dynamic mode decomposition to the Koopman operator, J. Nonlinear Sci. **28**, 687 (2018).

[45] J. H. Tu, C. W. Rowley, D. M. Luchtenburg, S. L. Brunton, and J. N. Kutz, On dynamic mode decomposition: Theory and applications, J. Comput. Dyn. **1**, 391 (2014).

[46] M. J. Colbrook, Another look at residual dynamic mode decomposition in the regime of fewer snapshots than dictionary size, Physica D **469**, 134341 (2024).

[47] M. J. Colbrook and A. Townsend, Rigorous data-driven computation of spectral properties of Koopman operators for dynamical systems, Commun. Pure Appl. Math. **77**, 221 (2024).

[48] L. N. Trefethen and M. Embree, *Spectra and Pseudospectra: The Behavior of Nonnormal Matrices and Operators* (Princeton University Press, Princeton, 2005).

[49] E. Ott and T. M. Antonsen, Low dimensional behavior of large systems of globally coupled oscillators, Chaos **18**, 037113 (2008).

[50] E. Ott and T. M. Antonsen, Long time evolution of phase oscillator systems, Chaos **19**, 023117 (2009).

[51] S. H. Strogatz, R. E. Mirollo, and P. C. Matthews, Coupled nonlinear oscillators below the synchronization threshold: Relaxation by generalized Landau damping, Phys. Rev. Lett. **68**, 2730 (1992).

[52] N. Nakagawa and Y. Kuramoto, Collective chaos in a population of globally coupled oscillators, Prog. Theor. Phys. **89**, 313 (1993).

[53] J. Kadmon and H. Sompolinsky, Transition to chaos in random neuronal networks, Phys. Rev. X **5**, 041030 (2015).

[54] F. Mastrogiuseppe and S. Ostojic, Linking connectivity, dynamics, and computations in low-rank recurrent neural networks, Neuron **99**, 609 (2018).

[55] S. L. Brunton, B. W. Brunton, J. L. Proctor, E. Kaiser, and J. N. Kutz, Chaos as an intermittently forced linear system, Nat. Commun. **8**, 19 (2017).

[56] G. A. Gottwald and F. Gugole, Detecting regime transitions in time series using dynamic mode decomposition, J. Stat. Phys. **179**, 1028 (2020).

[57] J. N. Kutz, J. L. Proctor, and S. L. Brunton, Applied Koopman theory for partial differential equations and data-driven modeling of spatio-temporal systems, Complexity **2018**, 6010634 (2018).

[58] Y. Yin, C. Kou, S. Jia, L. Lu, X. Yuan, Y. Luo, PCDMD: Physics-constrained dynamic mode decomposition for accurate and robust forecasting of dynamical systems with imperfect data and physics, Comput. Phys. Commun. **304**, 109303 (2024).

[59] S. T. Dawson and S. L. Brunton, Improved approximations to Wagner function using sparse identification of nonlinear dynamics, AIAA J. **60**, 1691 (2022).